Computers and Chemical Engineering 72 (2015) 210–221

Contents lists available at ScienceDirect

Computers and Chemical Engineering

journal homepage: www.elsevier.com/locate/compchemeng

MINLP model for the detailed scheduling of refined products pipelines with flow rate dependent pumping costs

Vanina G. Cafaro, Diego C. Cafaro, Carlos A. Méndez, Jaime Cerdá *

INTEC (UNL – CONICET), Güemes 3450, 3000 Santa Fe, Argentina

ARTICLE INFO

Article history:
Received 20 January 2014
Received in revised form 2 May 2014
Accepted 7 May 2014
Available online 22 May 2014

Keywords:
Multiproduct pipeline
Detailed scheduling
MINLP approach
Friction head loss
DICOPT solver

ABSTRACT

Multiproduct pipelines transport fuels from refineries to distant distribution terminals in batches. The energy needed to move the fluids through the pipeline is mainly associated with elevation gradients and friction head loss. Commonly, friction loss is the major term requiring pump stations to keep the flow moving, and it is strongly dependent on the fluid flow rate. Some studies have been carried out for reducing the pumping costs in multiproduct pipelines, but none of them has been focused on thoroughly considering the head loss due to friction along the pipeline. This paper introduces a novel MINLP continuous-time formulation for the detailed scheduling of single-source pipelines, rigorously tracking power consumption at every pipeline segment through nonlinear equations. Real-world case studies are successfully solved using GAMS–DICOPT algorithm, which proves to be a useful tool for solving large-scale, nonlinear scheduling problems. Important reductions in the operation costs are achieved by keeping a more stable flow rate profile over the planning horizon.

1. Introduction

Refined products pipelines begin at refineries and end at distribution terminals. These terminals are collections of large tanks located along the pipeline near customers' facilities. Oil products move down the pipeline in batches, which are pumped at the refinery and delivered to the terminals once they reach their outlet sections. Sometimes the entire flow is diverted into one terminal, while in other cases only a splitstream is discharged and the remaining flow continues moving forward. Refined products are then transported from terminals to retail outlets or commercial and industrial customers by tank trucks or rail cars.

Pipelines transport fluids from one point of higher energy to other point of lower energy, unless something like a closed valve stops the flow. In pipelines, energy is normally measured as pressure. When energy is added to a fluid by a pump or compressor, pressure builds. Although a fluid would seem to be slippery by its nature, friction must still be considered. Friction between the internal walls of the pipeline and the fluid, as well as the intrinsic friction between the molecules of the fluid, resist the flow and must be overcome with energy (Miesner and Leffler, 2006). Friction generates heat, which is another way of saying that it converts pressure energy into heat. This heat is transferred to the fluid and the surrounding environment. Moreover, gravity adds or subtracts pressure depending on the elevation profile.

1.1. Fluid dynamics of a liquid pipeline

The equation for the pressure of an incompressible flow at two different points 1 and 2 along a single pipeline is given by the Bernoulli's principle (1), which can be derived from the principle of conservation of energy (Bernoulli, 1738).

$$z_1 + \frac{p_1}{\rho g} + \frac{v_1^2}{2g} + H_P = z_2 + \frac{p_2}{\rho g} + \frac{v_2^2}{2g} + h_L + H_T \quad (1)$$

The first term in Eq. (1) stands for the elevation head, the second term is the pressure head, and the third term accounts for the velocity head. Moreover, H_P and H_T represent the pump head addition and turbine head subtraction, while h_L is the head loss due to friction along the segment connecting points 1 and 2. All these terms are typically measured in meters. Parameter g is the gravity acceleration (9.81 m/s^2), and ρ is the fluid density.

For long-distance pipelines, friction loss is the major term requiring pump stations to keep the flow moving. Friction loss is dictated by several factors: fluid viscosity, density, mean velocity, pipeline length and roughness of the internal walls of the pipeline. But it is particularly sensitive to the fluid flow rate. However, no

* Corresponding author. Tel.: +54 342 4559175; fax: +54 342 4550944.
E-mail addresses: cmendez@intec.unl.edu.ar (C.A. Méndez), jcerda@intec.unl.edu.ar (J. Cerdá).

http://dx.doi.org/10.1016/j.compchemeng.2014.05.012
0098-1354/

Nomenclature

Sets

I	ordered set of batches ($I^{old} \cup I^{new}$)
I^{new}	set of new batches to be injected during the planning horizon
I^{old}	set of old batches in the pipeline at the beginning of the time horizon
J	set of terminals/pipeline segments
$J_{i,i}$	subset of depots demanding product from batch i while injecting lot i'
K	ordered set of detailed operations
K_i	subset of detailed operations taking place during the injection of batch i

Parameters

ca	unit flow restart cost
cp	unit pumping cost
cs	unit flow stoppage cost
d_j	diameter of pipeline segment j
d_{min}	minimum delivery size for a single cut
$dd_{i,j}^{(i')}$	aggregate delivery from batch i to terminal j during the injection of batch i'
fco	fixed cost for performing a multi-cut operation
$ft_{i'}$	completion time for the injection of batch i'
l_j	length of segment j
l_{min}/l_{max}	minimum/maximum length of a detailed run
pv	total pipeline volume
$qq_{i'}$	overall size of the new lot i'
r_j	absolute roughness for each segment
$st_{i'}$	starting time for the injection of batch i'
z_j	elevation of terminal j (z_0 is the refinery elevation)
$\varepsilon_1/\varepsilon_2$	small values
η	pump yield factor
μ	average dynamic viscosity of the fluid
ρ	average liquid density
σ_j	volumetric coordinate of depot j from the origin of the pipeline
u	mean velocity of products flowing into the pipeline
ν	average kinematic viscosity

Variables: positive variables

AV_k	activated volume to perform operation k
C_k	completion time of the detailed operation k
$D_{i,j}^{(k)}$	volume of batch i delivered to terminal j during run k
$EC_{j,k}$	energy consumed at each pipeline segment j during the detailed operation k
FAT_k	farthest active terminal receiving product during operation k
$F_i^{(k)}$	upper coordinate of batch i at the end of operation k
L_k	length of the detailed operation k
$p_{j,k}$	pump power required for transporting product into the pipeline segment j during operation k
Q_k	volume injected at the oil refinery during run k
$q_{j,k}$	pump rate through segment j during operation k (m^3/s)
SV_k	stopped volume to perform operation k
$T_{j,k}$	volume pumped through segment j while performing the operation k
$W_i^{(k)}$	content of lot i at the completion of operation k

Binary variables

u_k	denoting that operation k is executed whenever $u_k = 1$
$x_{i,j}^{(k)}$	indicating that a portion of batch i is delivered to depot j during operation k if $x_{i,j}^{(k)} = 1$
$y_j^{(k)}$	equals 1 if the segment j is active during run k

previous work on the scheduling of refined products pipelines has rigorously considered this aspect. This work presents an extension of a previous optimization model (Cafaro et al., 2012) that overcomes such a limitation.

2. Literature review

Most contributions on pipeline scheduling have been proposed to find the optimal sequence of batch injections in multiproduct pipelines conveying liquid products from a single refinery to several destinations. Hane and Ratliff (1995) propose a discrete model to generate cyclic pipeline schedules which can be easily priced out in a branch-and-bound algorithm. Later on, Rejowski and Pinto (2003) develop a discrete-time MILP model for the scheduling of single pipelines, focusing on the convenience of intermittent operation. The intermittent operation is desirable to avoid working during peak electricity periods given that pumping costs may present a five-fold increase with respect to their normal values.

Recent works in the field of multiproduct pipeline scheduling are focused on pipeline networks with more complex structures. García-Sánchez et al. (2008) develop a hybrid methodology that combines tabu search and discrete-event simulation for the scheduling of pipeline systems with branching terminals. Lopes et al. (2010) introduce a hybrid framework for the scheduling of mesh-like pipeline networks with several alternative paths to move batches from the entry point to the assigned destinations. Boschetto et al. (2010) develop a hierarchical decomposition technique, primarily based on the work of Neves et al. (2007). The main goal is to determine the exact times to pump products into the pipelines given a set of operations predefined by a heuristic module. The approach was applied to a large real-world pipeline network transporting 15 products. Herrán et al. (2010) present a discrete mathematical approach for the short-term scheduling of a multi-pipeline transportation system with reversible segments.

Contrarily to discrete models, continuous-time MILP representations have proved to be an efficient way to find the optimal transportation plan for single pipelines (Cafaro and Cerdá, 2004; Relvas et al., 2006), tree-structure pipeline networks (Castro, 2010; MirHassani and Jahromi, 2011; Cafaro and Cerdá, 2011) and mesh-structure pipeline networks (Cafaro and Cerdá, 2012). These approaches provide the set of batch stripping operations to be diverted to the distribution terminals during every pumping run, but they neither specify the detailed sequence of individual cuts to be performed by the pipeline operator nor the flow rate profile at every pipeline segment. In response to this need, recent approaches have been proposed for generating the detailed pipeline schedule. Cafaro et al. (2011) present two alternative tools. One of them is based on a rigorous MILP mathematical formulation, and the other one relies on a discrete-event simulation model assessing a series of heuristic rules. Both approaches assume that only one terminal can receive material from the line while a batch injection is performed. Later on, the same authors extend their MILP formulation by allowing parallel deliveries to more than one depot during the same injection (Cafaro et al., 2012). The proposed formulation constitutes a more realistic representation of daily pipeline operations that is able to keep the stream flow rate within a specific range in

each pipeline segment by properly controlling the delivery sizes at intermediate offtake stations. Considerable savings in both CPU times and operation costs are achieved. All these representations aim to minimize the operation costs based on reducing the number of pipeline segment stoppages, yielding reductions in energy consumption and pump maintenance costs.

Although detailed scheduling models show interesting results like increasing the number of simultaneous deliveries to keep the segments almost always active, they do not rigorously calculate energy consumption due to fluid friction loss. Modeling friction loss in pipeline scheduling problems is a challenging task. Rejowski and Pinto (2005) extend their previous approach by adopting approximate nonlinear functions of the pump power with regards to the pipeline flow rate. Afterwards, the same authors present an MINLP formulation based on a continuous-time representation, assuming that the pipeline operates intermittently and the pumping costs depend on the yield rate of booster stations, which in turn may operate at different flow rate ranges (Rejowski and Pinto, 2008).

In a more recent work, Cafaro et al. (2013) propose an MILP model where pumping costs due to friction are estimated by introducing a piecewise linear function of the flow rate. Despite being an approximate method, it yields important reductions in operation costs with regards to previous contributions. Nonetheless, more accurate energy cost estimations are still pending. This manuscript presents a novel MINLP continuous formulation for developing the detailed schedule of single-source pipelines, allowing simultaneous deliveries to multiple terminals, while rigorously tracking energy consumption due to friction. We propose to use the implicit Colebrook–White equation (Colebrook and White, 1937) to precisely calculate the power required to transport the fluid inside each segment of the pipeline. The new approach is applied to a real-world case study, using GAMS–DICOPT as the MINLP solver (Durán and Grossmann, 1986), to evaluate the model performance and the quality of the results.

3. Problem assumptions

The MINLP formulation presented throughout this work relies on the following assumptions:

(1) A single-source pipeline with multiple terminals and unidirectional flow is considered.
(2) The pipeline is full of incompressible liquid products at any time.
(3) The aggregate transportation plan (product sequence, batch size and destination) is given beforehand.
(4) An admissible flow rate range is specified for each pipeline segment.
(5) Batches move into the pipeline in plug flow. Interface or "transmix" volumes are neglected.
(6) The detailed schedule comprises a sequence of individual operations, each one characterized by a single batch injection and one or multiple simultaneous deliveries.
(7) If a terminal receives product during an individual operation, the product must be taken from a single batch.
(8) The mean velocity (u) is obtained from the ratio between the pump rate (q) and the pipeline section: $u = 4q/\pi d^2$. As a result, the Reynolds number is $Re = 4q/\pi d\nu$, with ν being the fluid kinematic viscosity.
(9) Refined products flow in turbulent regime into the pipeline segments. In other words, the Reynolds number is greater than 4000. For the examples solved in this work, the Reynolds number is greater than 4×10^5 at every pipeline segment, even in the worse condition, i.e. at the minimum pumping rate.
(10) The relationship between the head loss due to friction (h_L) and the pump rate (q) in a pipeline segment of length l and diameter d is derived from the Darcy's equation (2) (Darcy, 1857). It introduces the dimensionless friction factor f, also known as the Fanning factor.

$$h_L = f\frac{l}{d}\frac{u^2}{2g} = f\frac{l}{d}\frac{q^2}{2g}\left[\frac{4}{\pi d^2}\right]^2 = 8f\frac{l}{d^5}\frac{q^2}{g\pi^2} \tag{2}$$

Only a few special problems in fluid mechanics can be entirely solved by rational mathematical means; all other problems require methods of solution which rest, at least in part, on experimentally determined coefficients. Because of the great variety of fluids being handled in modern industrial processes, a single equation like the Darcy's formula, which can be used for the flow of any fluid into pipelines, offers obvious advantages. Such an equation can be derived rationally from dimensional analysis.

(11) From assumption 9 (turbulent flow regime), the friction factor f can be calculated through the Colebrook–White equation (3).

$$\frac{1}{\sqrt{f}} = -2\ \log_{10}\left(\frac{(r/d)}{3.7} + \frac{2.51}{Re\sqrt{f}}\right) \tag{3}$$

Eq. (3) is an implicit function accounting for two contributions: the pipeline roughness (r), and the flow turbulence given by the Reynolds number, Re. This equation is usually shown in the well-known Moody's diagram (Moody, 1944).

(12) The electric power to drive a pump depends on the flow rate, the liquid density and the differential height (H_p). If it is given in kilowatts (kW), it can be derived from: $P = H_p q\rho g/\eta 10^3$. Parameter η is the pump yield rate, which is assumed to be independent of the pump rate.

(13) For simplicity, we assume constant physical properties (namely density and viscosity) of an average oil product transported through the pipeline system, so that the only variable determining the friction factor f at every segment is the flow rate (q). Hence, the power required to compensate for the friction loss (P_L) is given by Eq. (4), representing a non-linear function rapidly growing with q.

$$P_L = \frac{h_L q\rho g}{\eta 10^3} = \frac{8fq^2 l}{\pi^2 d^5 g}\frac{g\rho q}{\eta 10^3} = \frac{8fq^3 l}{\pi^2 d^5}\frac{\rho}{\eta 10^3} = \frac{8\rho}{\pi^2\eta 10^3}\frac{l}{d^5}fq^3 \tag{4}$$

Clearing $1/\sqrt{f}$ from the previous equation yields:

$$\frac{1}{\sqrt{f}} = \left(\frac{8\rho}{\pi^2\eta 10^3}\frac{l}{d^5}\frac{q^3}{P_L}\right)^{1/2} \tag{5}$$

Finally, replacing (5) and the Reynolds number expression in Eq. (3) we obtain an implicit equation relating the pump power and the flow rate.

$$\left(\frac{8\rho}{\pi^2\eta 10^3}\frac{l}{d^5}\frac{q^3}{P_L}\right)^{1/2} = -2\ \log_{10}\left[\frac{(r/d)}{3.7} + 2.51\frac{\pi d\nu}{4q}\left(\frac{8\rho}{\pi^2\eta 10^3}\frac{l}{d^5}\frac{q^3}{P_L}\right)^{1/2}\right]$$

$$= -2\log_{10}\left(\frac{(r/d)}{3.7} + \frac{2.51}{4}\nu\sqrt{\frac{8l\rho}{d^3\eta 10^3}}\frac{q^{1/2}}{P_L{}^{1/2}}\right) \tag{6}$$

This implicit equation is introduced in the MINLP mathematical model in order to calculate the energy consumption in every pipeline segment.

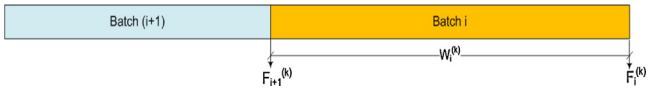

Fig. 1. Relation between the frontal coordinates of successive batches at the end of run k.

4. Mathematical formulation

In this section we present the MINLP optimization model providing an efficient detailed schedule of delivery operations, taking into account the energy consumption at pump stations, based on the rigorous calculation of the friction loss as a function of the flow rate through every pipeline segment.

4.1. Sets

The detailed scheduling model involves five major sets: the set of detailed operations (K) chronologically arranged, representing the sequence of batch injections to be performed by the pipeline operator; the set of terminals (J) and pipeline segments (J'); the set of new batches to be injected (I^{new}) and those batches inside the pipeline at the beginning of the time horizon (I^{old}). Batches in the set $I = I^{old} \cup I^{new}$ are arranged in the same order that they move into the pipeline.

4.2. Variables

Similar to previous approaches proposed by Cafaro et al. (2011, 2012), the model comprises a series of continuous variables controlling the time and volume of new product injections, and tracking the size and location of the batches into the pipeline: L_k is the length of the detailed operation k, C_k its completion time, Q_k is the volume injected during run k, while $W_i^{(k)}$ and $F_i^{(k)}$ are the content and frontal coordinate of lot i at the completion of operation k, respectively. Because lot $(i+1)$ is introduced immediately after batch i into the line, it moves right behind batch i all along the pipeline (see Fig. 1). Besides, new continuous variables are introduced in the mathematical formulation accounting for the flow rate, friction loss and pump power at every pipeline segment. $T_{j,k}$ is the total volume pumped through segment j while performing the operation k, $q_{j,k}$ is the corresponding pump rate, while $EC_{j,k}$ is the required power to keep the flow moving.

Binary variables are also required to denote that operation k is effectively executed (whenever $u_k = 1$), to determine if segment j is active during run k (in case $y_{j,k} = 1$), and if a portion of the batch i is delivered to depot j during operation k (every time $x_{i,j}^{(k)} = 1$).

4.3. Constraints

The proposed formulation involves, on the one hand, a typical block of linear constraints determining the sequence of detailed scheduling operations first introduced by Cafaro et al. (2012) and, on the other hand, novel nonlinear equations standing for the friction loss calculation and the corresponding energy consumption.

4.3.1. Detailed scheduling of delivery operations

4.3.1.1. Start and end times of the detailed operation k. Since pumping operations are chronologically arranged, Eqs. (7)–(9) should be satisfied.

$$C_k \le ft_{i'} \quad \forall i' \in I^{new}, \quad k = last(K_{i'}) \tag{7}$$

$$C_k - L_k \ge C_{k-1} \quad \forall k \in K \tag{8}$$

$$C_k - L_k \ge st_{i'} \quad \forall i' \in I^{new}, \quad k = first(K_{i'}) \tag{9}$$

The subset $K_{i'} \subseteq K$ stands for the string of input operations required to pump the whole new batch $i' \in I^{new}$ into the pipeline. $st_{i'}$ and $ft_{i'}$ are the start and end times of the injection of batch i' (given data). From the chronological viewpoint, the pumping operation $(k-1) \in K$ immediately precedes run k. Moreover, it is said that the element $k \in K$ is a dummy run if it is never executed. Though the cardinality of every subset $K_{i'}$ is not known beforehand, a conservative estimate of $|K_{i'}|$ is given by the number of aggregate deliveries to be accomplished during the injection of batch i'.

Moreover, fictitious operations featuring null length at the optimum must be placed at the end of the run sequence, to avoid solution degeneracy.

$$l_{\min} u_k \le L_k \le l_{\max} u_k \quad \forall i' \in I^{new}, \quad k \in K_{i'} \tag{10}$$

$$u_k \le u_{k-1} \quad \forall i' \in I^{new}, \quad k \in K_{i'}, \quad k > first(K_{i'}) \tag{11}$$

4.3.1.2. Tracking batch size and location. Batches inside the pipeline are monitored at the end of each operation. Eqs. (12)–(14) represent the relationship between the front/back coordinates of adjacent batches at the end of run k. The size of lot i at the end of operation k ($W_i^{(k)}$) can be computed by subtracting the amount delivered from batch i to all the terminals $j \in J$ during run k ($D_{i,j}^{(k)}$) and adding the volume Q_k, if the batch i is the one being injected during run k.

$$F_{i+1}^{(k)} + W_i^{(k)} = F_i^{(k)} \quad \forall i \in I, \quad i' \in I^{new}, \quad i' > i, \quad k \in K_{i'} \tag{12}$$

$$W_i^{(k)} = W_i^{(k-1)} - \sum_{j \in J_{i,i'}} D_{i,j}^{(k)} \quad \forall i \in I, \quad i' \in I^{new}, \quad i' > i, \quad k \in K_{i'} \tag{13}$$

$$F_{i'}^{(k)} = W_{i'}^{(k)} = W_{i'}^{(k-1)} + Q_k - \sum_{j \in J_{i',i'}} D_{i',j}^{(k)} \quad \forall i' \in I^{new}, \quad k \in K_{i'} \tag{14}$$

In Eq. (14) the subset $J_{i,i'}$ comprises those terminals that are planned to receive a portion of batch i during the injection of batch i'. Moreover, $W_{i'}^{(k-1)} = 0$ for $k = \text{first}\,(k_{i'})$

4.3.1.3. Imposing conditions for product deliveries. Linear constraints (15)–(18) control the feasibility of delivery operations.

$$d_{\min} x_{i,j}^{(k)} \le D_{i,j}^{(k)} \le dd_{i,j}^{(i')} x_{i,j}^{(k)} \quad \forall i \in I, \quad i' \in I^{new}, \quad i' \ge i, \quad j \in J_{i,i'}, \quad k \in K_{i'} \tag{15}$$

$$F_i^{(k-1)} \ge \sigma_j x_{i,j}^{(k)} \quad \forall i \in I, \quad i' \in I^{new}, \quad i' \ge i, \quad j \in J_{i,i'}, \quad k \in K_{i'} \tag{16}$$

$$F_i^{(k)} - W_i^{(k)} \le \sigma_j + (pv - \sigma_j)(1 - x_{i,j}^{(k)}) \quad \forall i \in I, \quad i' \in I^{new}, \quad i' > i, \quad j \in J_{i,i'}, \quad k \in K_{i'} \tag{17}$$

$$\sum_{i \in I : j \in J_{i,i'}} x_{i,j}^{(k)} \le u_k \quad \forall i' \in I^{new}, \quad k \in K_{i'}, \quad j \in J \tag{18}$$

Constraint (15) imposes lower and upper bounds on the size of the product deliveries. The parameter d_{min} is the minimum size for a batch delivery during a single operation, whereas $dd_{i,j}^{(i')}$ is the size of the planned aggregate delivery to terminal j during the injection of batch i'. It is also necessary to set up the feasible conditions for a product delivery through constraints (16)–(18). To divert some product from the pipeline to depot j, the front coordinate of batch i at the end of run k must never be lower than the depot location σ_j. Moreover, the backcoordinate of batch i at the start of run k should be lower than σ_j by at least the volume $D_{i,j}^{(k)}$ delivered to terminal j during run $k \in K_{i'}$. Parameter pv is the total pipeline volume.

If one of the feasibility conditions cannot be satisfied, Eqs. (16) and (17) become redundant by making $x_{i,j}^{(k)} = 0$, and because of Eq. (15), the related product delivery is null ($D_{i,j}^{(k)} = 0$).

4.3.1.4. Input/output volume balance. Due to liquid incompressibility, an exact balance between input and output volumes at every operation k is enforced.

$$\sum_{\substack{i \in I \\ i \le i'}} \sum_{j \in J_{i,i'}} D_{i,j}^{(k)} = Q_k \quad i' \in I^{new}, \quad k \in K_{i'} \tag{19}$$

4.3.1.5. Fulfillment of the batch transportation plan. The total volume injected into the pipeline and the total amount diverted from every batch $i \le i'$ over all the detailed operations should fulfill the aggregate plan, given beforehand by parameters $qq_{i'}$ (the overall size of the new lot i') and $dd_{i,j}^{(i')}$ (the aggregate delivery from batch i to terminal j during the injection of batch i')

$$\sum_{k \in K_{i'}} D_{i,j}^{(k)} = dd_{i,j}^{(i')} \quad \forall i \in I, \quad i' \in I^{new}, \quad i' \ge i, \quad j \in J_{i,i'} \tag{20}$$

$$\sum_{k \in K_{i'}} Q_k = qq_{i'} \quad \forall i' \in I^{new} \tag{21}$$

4.3.1.6. Active and idle pipeline segments. Constraints (22) and (23) determine the value of variable $y_{j',k}$ deciding on the activation of segment j' during run k.

$$y_{j'}^{(k)} \ge \sum_{i \in I : j \in J_{i,i'}} x_{i,j}^{(k)} \quad \forall i' \in I^{new}, \quad j' \in J', \quad j = j', \quad k \in K_{i'} \tag{22}$$

$$y_{j'}^{(k)} \le \sum_{i \in I} \sum_{\substack{j \ge j' \\ j \in J_{i,i'}}} x_{i,j}^{(k)} \quad \forall i' \in I^{new}, \quad j' \in J', \quad k \in K_{i'} \tag{23}$$

$$y_{j'-1}^{(k)} \ge y_{j'}^{(k)} \quad \forall j' > 1, \quad k \in K \tag{24}$$

Inequality (22) states that every segment j' supplying terminal $j = j'$ is active if terminal j receives product from the pipeline during run k. On the contrary, if no terminal $j \ge j'$ receives product from the pipeline at operation k, segment j' is idle, as imposed by constraint (23). Finally, constraint (24) makes all the segments preceding an active segment to be also active.

4.3.1.7. Identifying the farthest active terminal. The coordinate of the farthest terminal receiving product from the line at every run k (FAT_k) is calculated through constraints (25) and (26).

$$FAT_k \ge \sigma_j y_j^{(k)} \quad \forall j \in J, \quad k \in K \tag{25}$$

$$FAT_k \le \sigma_j + (pv - \sigma_j) y_{j+1}^{(k)} \quad \forall j \in J, \quad k \in K \tag{26}$$

Based on the value of variable FAT_k at two successive operations, stopped and activated volumes (represented by variables AV_k and SV_k) can be readily obtained. To evaluate the quality of the detailed schedule, the notion of total activated volume (AV) is introduced. AV is the accumulated volume of idle pipeline segments where the fluid motion should be restored to carry out downstream delivery operations, throughout the planning horizon. An equivalent criterion is the total stopped volume (SV) representing the accumulated volume of active segments where the flow is stopped. Their values are lower-bounded through Eqs. (27)–(29).

$$AV_k \ge FAT_k - FAT_{k-1} \quad \forall k \in K_{i'}, \quad k > 1, \quad i' \in I^{new} \tag{27}$$

$$SV_k \ge FAT_{k-1} - FAT_k + \sigma_{TA} \quad \forall i' \in I^{new}, \quad k \in K_{i'}, \quad k > 1, \quad i' \in I^{new} \tag{28}$$

$$SV_k \ge FAT_k + \sigma_{TA} \quad \forall i' \in I^{new}, \quad k \in K_{i'}, \quad k = 1, \quad i' \in I^{new} \tag{29}$$

Parameter σ_{TA} is the volumetric coordinate of the current active terminal at $t = 0$.

4.3.2. Friction loss and energy consumption

4.3.2.1. Measuring pumping energy to compensate for the friction loss. The volume pumped through each pipeline segment j' ($T_{j',k}$) is exactly equal to the overall quantity of product delivered to downstream terminals $j \ge j'$.

$$T_{j',k} = \sum_{i \in I} \sum_{\substack{j \in J_{i,i'} \\ j \ge j'}} D_{i,j}^{(k)} \quad \forall i' \in I^{new}, \quad k \in K_{i'}, \quad j' \in J' \tag{30}$$

As a result, the flow rate at every segment (in m^3/s) is estimated by:

$$q_{j',k} = \frac{T_{j',k}}{(L_k + \varepsilon_1)3600} + \varepsilon_2 \tag{31}$$

where ε_1 and ε_2 are very small values, introduced to avoid computational failures of the NLP solvers. They are measured in h and m^3/s, respectively.

From the Darcy's and Colebrook–White's equations, we introduce an implicit function of the pump power due to friction ($p_{j',k}$) and the flow rate ($q_{j',k}$) moving through the segment j' during operation k.

$$\left(\frac{8 l_{j'} \rho}{d_{j'}^5 \eta \pi^2 10^3}\right)^{1/2} \frac{q_{j',k}^{3/2}}{p_{j',k}^{1/2}} = -2 \log_{10}\left(\frac{r_{j'}/d_{j'}}{3.7}\right) + \frac{2.51}{4} \nu \sqrt{\frac{8 l_{j'} \rho}{d_{j'}^3 \eta 10^3}} \frac{q_{j',k}^{1/2}}{p_{j',k}^{1/2}} \quad \forall j' \in J', \quad k \in K \tag{32}$$

As a result, the energy consumed at every pipeline segment j' ($EC_{j',k}$, in kWh) comprises one term due to the friction loss and a second term accounting for elevation differences between successive terminals $j-1$ and j, i.e. $(z_j - z_{j-1})$.

$$EC_{j',k} = p_{j',k} L_k + T_{j',k} \rho g (z_j - z_{j-1}) \quad \forall j' \in J', \quad j = j', \quad k \in K \tag{33}$$

Note that the first term of Eq. (33) is bilinear. Eqs. (31)–(33) give rise to a non-convex model, whose resolution is certainly complex.

4.4. Objective function

The problem goal is to develop a detailed pipeline schedule that meets the aggregate transportation plan at minimum energy consumption and restart/stoppage costs. That is to say:

$$Min \quad z = \sum_{k \in K} cp\left(\sum_{j} EC_{j,k}\right) + ca\, AV_k + cs\, SV_k + fco\, u_k \tag{34}$$

In the objective function (34) parameter cp is the unit energy cost, ca/cs are the unit flow restart/stoppage costs, and fco is the fixed cost for performing each operation.

4.5. Solution strategy

The proposed MINLP formulation clearly yields a non-convex program, which hinders the problem convergence. In fact, searching for the optimal solution can be extremely costly. To save this drawback, a solution strategy is here presented. The aim is to obtain a feasible initial point to facilitate the MINLP convergence.

In the first step, the MILP model proposed by Cafaro et al. (2012) is solved to optimality to obtain the detailed schedule with minimum restart and stoppage volumes, but still not accounting for pumping costs. Then, the value of the discrete variables u_k, $y_j^{(k)}$ and $x_{i,j}^{(k)}$ is fixed, and a feasible solution for the proposed MINLP formulation is obtained by solving the first NLP sub-problem. Afterwards, all the discrete variables are unfixed, nonlinear equations are linearized, and the first MILP (master program) is solved to optimality. Following DICOPT procedure (Durán and Grossmann, 1986), new half-spaces linearizations and integer cuts are added at each iteration until the solution shows no further improvement. The proposed solution strategy is summarized in Fig. 2.

In this way, one can tackle the MINLP formulation by first solving an MILP program that finds out initial values for the discrete variables. The MINLP formulation is then solved using GAMS–DICOPT algorithm. DICOPT is based on the extensions of the outer-approximation algorithm for the equality relaxation strategy. The MINLP algorithm inside DICOPT solves a series of NLP and MILP sub-problems. These sub-problems can be solved using any solver that runs under GAMS (Brooke et al., 2006). In this case, we use CONOPT 3.15 and GUROBI 5.0.1, at the NLP and MILP solvers, respectively.

Although the algorithm has provisions to handle non-convexities, it does not necessarily obtain the global optimum. In this particular case, it is possible to use the configuration of the discrete variables obtained from the first MILP. Because it is a complex model, the integer-relaxed problem cannot be solved in a reasonable CPU time. However, NLP sub-problems with the integer variables fixed are much easier. As a reasonable integer configuration is known in advance, we can bypass the first relaxed NLP and directly start with the first integer configuration.

5. Results and discussion

In this section, three examples are solved using the proposed MINLP formulation accounting for flow rate dependent pumping costs, using an Intel Xeon Due-Processor (2.67 GHz) with 6 parallel threads. The first example deals with a single batch injection whose detailed delivery operations should be efficiently sequenced and scheduled. Next, the MINLP model is applied to an already known real-world pipeline system introduced by Rejowski and Pinto (2004), comprising a monthly time horizon. Finally, we divide the planning horizon into weekly schedules that are sequentially solved, one at a time. The solutions obtained are compared with the ones found when energy costs are not taken into account. Fig. 3 illustrates the pipeline system under study. It considers a pipeline of 925 km in length with segments of 20 and 14 in. in diameter, composed of one refinery at the origin and five depots. This pipeline transports almost 20% of Brazilian oil derivatives. Four liquid products (gasoline, diesel fuel, jet fuel and liquefied petroleum gases) are transported through the system, and five pipeline segments are identified (Ref.–D1, D1–D2, D2–D3, D3–D4, D4–D5). The same case study was addressed by Cafaro et al. (2012) with the aim of generating the detailed schedule that permits to minimize the flow restart and on/off pump switching costs.

At this planning instance, it is assumed that the set of batch injections (product sequence and batch sizes) is available. Fig. 4 shows the aggregate schedule given as input data for Examples 2 and 3, which was found by Cafaro and Cerdá (2008). The total length of the planning horizon is 660 h, and 49 batch deliveries must be optimally partitioned, sequenced and scheduled at this detailed operation level.

Table 1
Sizes and admissible flow-rate ranges for each pipeline segment.

Pipeline segment	Diameter (in.)	Length (km)	Flow rate range (m^3/h)
Refinery–D1	20	197.4	700–1200
D1–D2	20	123.4	600–1200
D2–D3	20	123.4	600–1200
D3–D4	20	296.2	600–1200
D4–D5	12	185.1	400–800

5.1. Example 1

Example 1 is an illustrative example showing the advantages of taking into account the flow rate dependent friction loss, which mostly determine pumping energy costs. It considers the injection of a single batch (B9) with 1235×10^2 m^3 of product P1 into the pipeline system (see line 5 of Fig. 4). The duct is initially filled with products $P4_{295}$, $P2_{1220}$, $P4_{120}$ (subscripts indicate batch volumes, in 10^2 m^3). By assumption, a common representative value of kinematic viscosity equal to 10^{-6} m^2/s and an average liquid density equal to 700 kg/m^3 are adopted. The diameter, the length and the admissible flow rates for every pipeline segment are all shown in Table 1. A pump yield factor of 0.9, and an absolute roughness of 0.002 inches for every pipeline segment are considered. Unit restart cost is set to 0.20 \$/m^3, each operation has a fixed cost of \$1000, while electricity driving centrifugal pumps has a unit cost of 0.20 \$/kWh.

The initial solution provided by the MILP model of Cafaro et al. (2012) is found in 0.562 CPUs, and is shown in Fig. 5. Such an approximate delivery schedule is included in the feasible region of the proposed MINLP formulation, constituting a valid initial point. After 3.346 CPUs and 4 major iterations of the MINLP optimization procedure (using DICOPT solver) we improve the solution 18.9% by reducing the total operation cost from \$86,651.11 to \$70,191.89. In particular, pumping costs are cut down by 29.4%. The optimal schedule of detailed operations is shown in Fig. 6. Note that the total number of operations and the restarted volumes remain unchanged, but the batch partitioning and flow rate profiles show significant improvement. The first detailed schedule found by the MILP formulation comprises five single withdrawals and only one operation (k_5) with three simultaneous deliveries to depots D1, D2 and D4 (see Fig. 5). In contrast, the optimized solution provided by the MINLP model comprises four simultaneous deliveries of a total of six runs, two of them supplying products to two depots in parallel, and other two diverting flows to three terminals during the same operation. The values over the dotted arrows in Figs. 5 and 6 represent the flow-rates (in 10^2 m^3/h) for every active segment. To reduce the power requirement, the MINLP solution presents a more stable behavior of the flow rates, avoiding high values especially in the last pipeline segment. Segment D4–D5 has a smaller diameter, which results in much higher friction loss. In fact, the total power required for operation k_4 in segment D4–D5 is 926.74 kW, while the first MILP solution yields a much higher value: 4731.41 kW. The pump power required at every pipeline segment to perform the optimized detailed schedule is shown in Table 2. The restart volume in the optimal solution amounts to 1235×10^2 m^3 ($400_{\text{Ref–D1}} + 250_{\text{D1–D2}} + 850_{\text{D2–D4}} + 135_{\text{D4–D5}}$, reactivated during operations k_1, k_2, k_3, and k_4, respectively). This

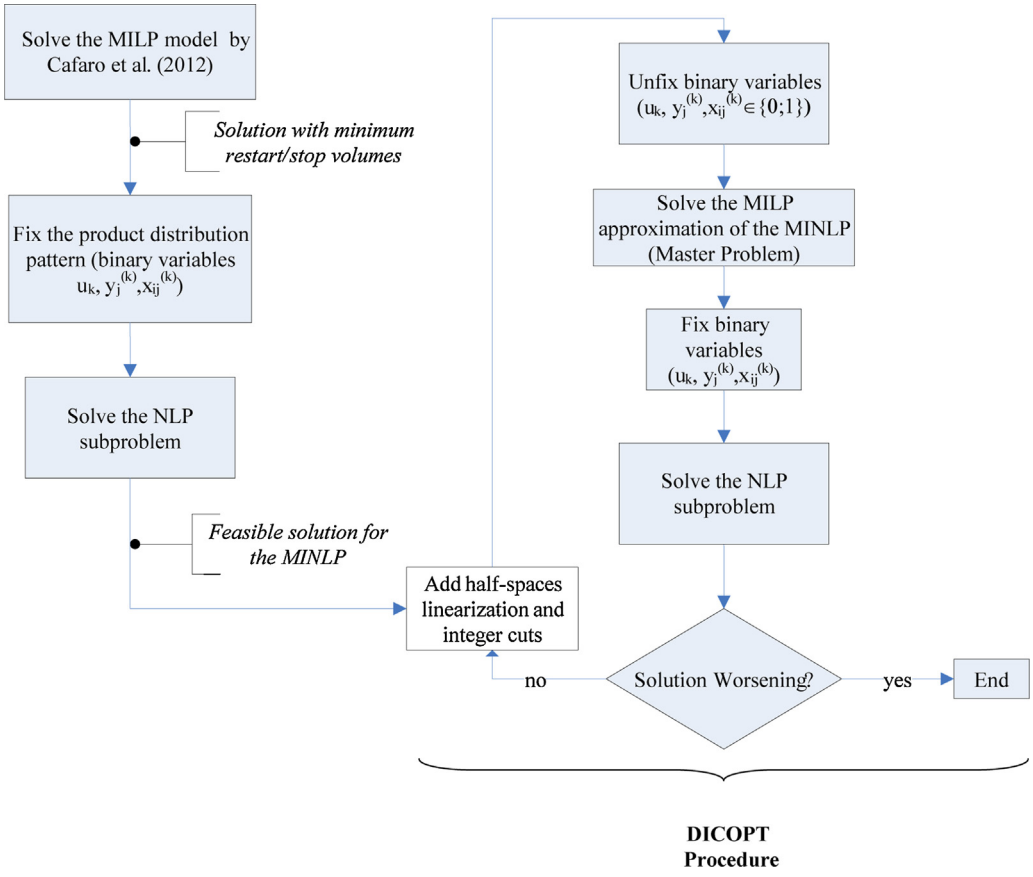

Fig. 2. Schematic diagram of the proposed solution strategy.

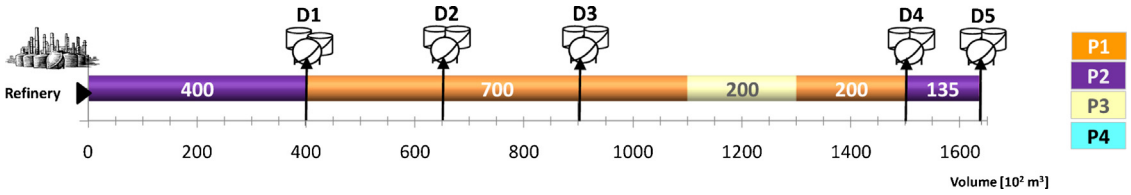

Fig. 3. Real-world pipeline system under study.

represents a restart cost of $24,700 (35% of the total operation cost). Other $39,421.9 correspond to pumping costs (56%), while the last 9% are fixed operation costs.

In order to find the global optimal solution for Example 1, we use GAMS/BARON 11.5.2 as the MINLP solver, but no feasible solution is found after 60,000 s of CPU time. To give an idea of the model complexity, we alternatively solve the reduced NLP model of Example 1 to global optimality, i.e. having fixed all the binary variables of the original MINLP to their initial values (step 3 of the solution strategy depicted in Fig. 2). In this case, the solution is found in 51.65 s with a relative gap of 10^{-4}, and the optimal cost is $80,848.6. In turn, using an NLP local optimizer (CONOPT 3.14), the sub-optimal solution amounts to $81,972.94, which is found in 0.41 CPUs.

Table 2
Optimal pump power required during the detailed operations of Example 1.

Detailed operation	Pump power required (kW) Pipeline segment				
	Ref.–D1	D1–D2	D2–D3	D3–D4	D4–D5
k_1	931.12				
k_2	575.39	359.69			
k_3	533.06	157.06	157.06	376.99	
k_4	533.06	157.06	157.06	376.99	926.74
k_5	551.89	341.26	157.06	376.99	
k_6	549.60	343.57	157.06		

5.2. Example 2

In this example, the monthly pipeline transportation plan is tackled all at once. By accounting for flow rate dependent pumping costs, it is expected a more stable pumping profile to carry out all the product deliveries compared to the solutions found by previous approaches only focused on restart/stop costs. The best detailed schedule obtained by solving the proposed MINLP continuous-time formulation is depicted in Fig. 7, and it is found in 18,428 CPUs. It comprises a sequence of 40 operations, injecting batches B6–B14 from the refinery. Overall, the MINLP detailed schedule comprises 31 simultaneous product withdrawals, i.e. dispatching more than one batch to the same number of terminals during a single operation. Of them, 20 operations supply products to two depots in

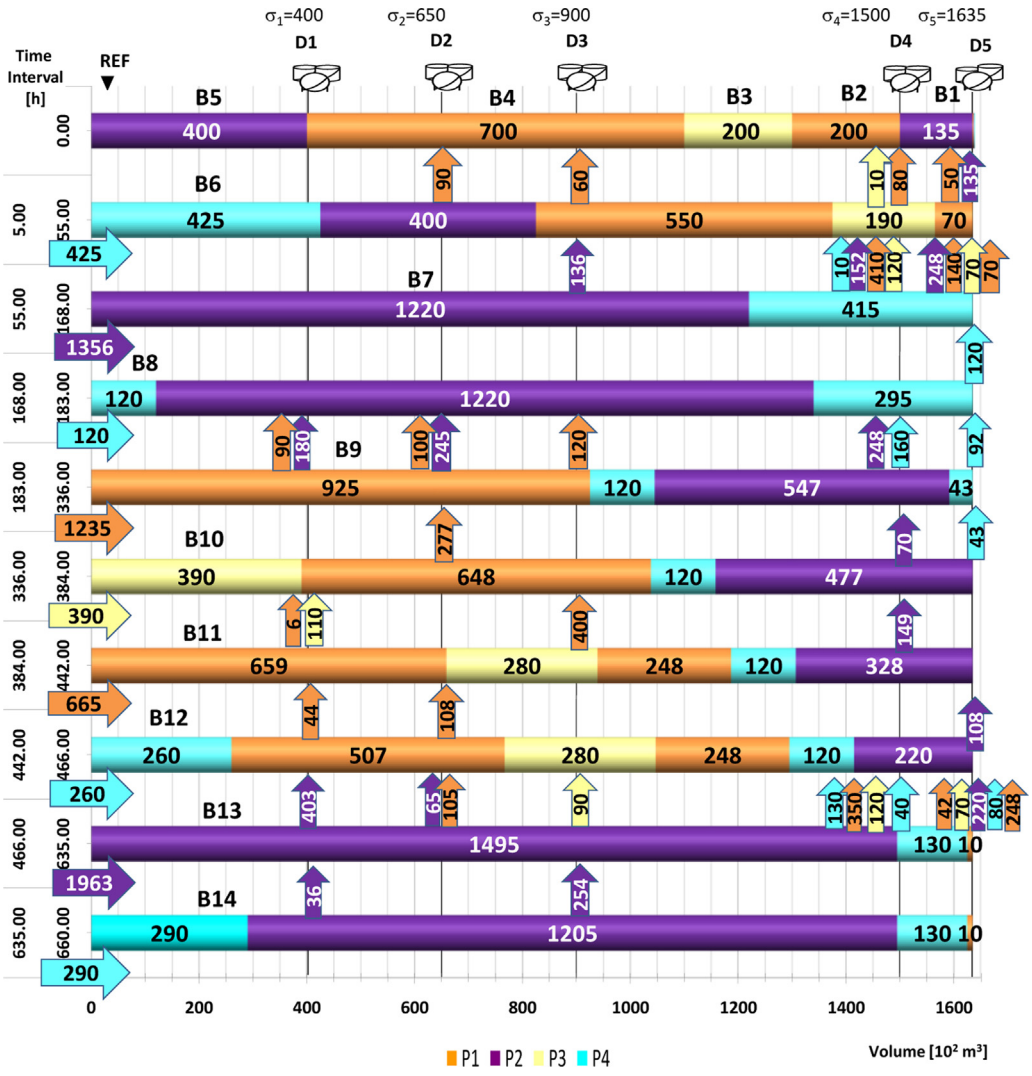

Fig. 4. Aggregate pipeline schedule for Examples 2 and 3.

parallel, 10 divert flows to three terminals simultaneously, and one operation (k_{35}) dispatches four batches to four depots at the same time. The remaining 9 operations perform single deliveries. Meanwhile, the first solution found by applying the MILP formulation also totalizes 40 operations, but they are executed in a totally different way: only one operation delivers products to three terminals simultaneously, 20 runs divert flows to two depots at the same time, and 19 cuts are performed individually.

From the total operation cost, it is concluded that the MINLP solution is much more efficient, sensitively reducing the friction loss and the associate pumping cost (see Table 3). With the new approach, the total operation cost ($726,431.44) is almost 12.5% less than that found by the previous approach (Cafaro et al., 2012), amounting to $830,332.46. With respect to the activated and stopped pipeline volumes over the planning horizon, both solutions are equivalent. Therefore, we demonstrate that the MINLP model also tends to reduce the flow restart cost as much as possible, but then the energy consumption can be significantly improved by stabilizing pumping rates at every pipeline segment.

Table 3
Model sizes, computational requirements and results for Examples 1, 2 and 3.

Ex.	Detailed oper. $\|K\|$	New batches	Weeks	Activated volume (10^2 m^3)	CPU time[a] (s)	Cont. vars.	Binary vars.	Eqs.	Total cost ($)
1	6	B9	–	1235	3.346	2253	84	1064	70,191.9
2	40	B6–B14	t_1–t_4	5845	18,428	15,085	567	7211	726,431.4
3	13	B6–B7	t_1	1770	21.5	4820	183	2233	277,507.5
	7	B8–B9	t_2	1235	2.3	2620	91	1204	98,869.3
	8	B10–B12	t_3	1720	1.3	3001	76	1303	118,303.1
	12	B13–B14	t_4	1120	74.1	4650	217	2517	231,883.5

[a] Overall time of the solution strategy. Models of Examples 1, 2 and 3 were also run using the GAMS/BARON 11.5.2 global optimizer, but no feasible solution was found after 60,000 s of CPU time.

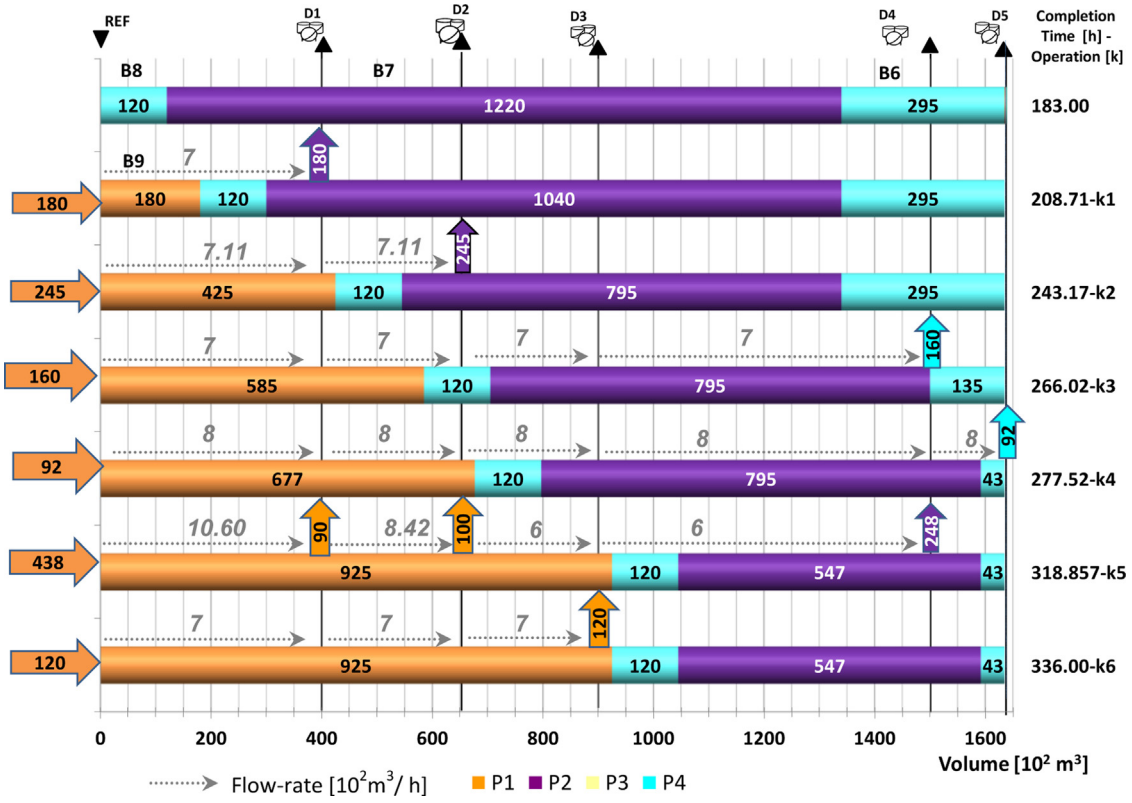

Fig. 5. Detailed delivery schedule obtained with the MILP formulation.

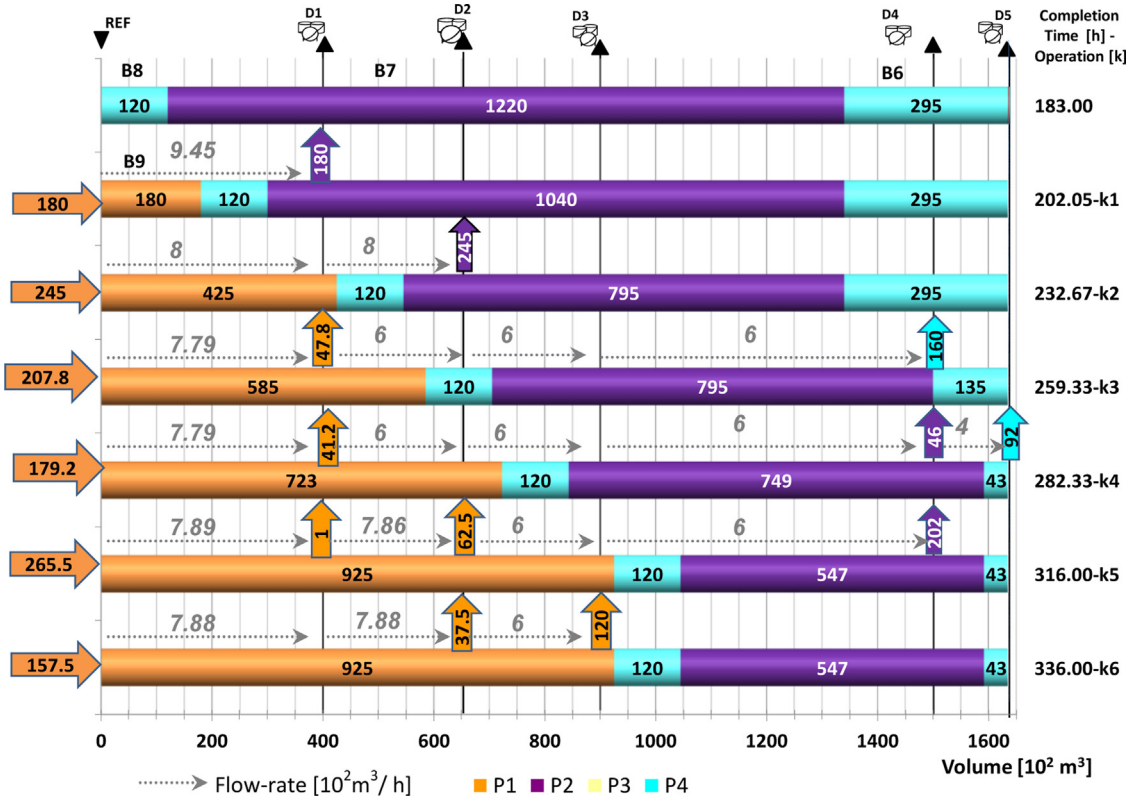

Fig. 6. Detailed delivery schedule obtained with the new MINLP formulation.

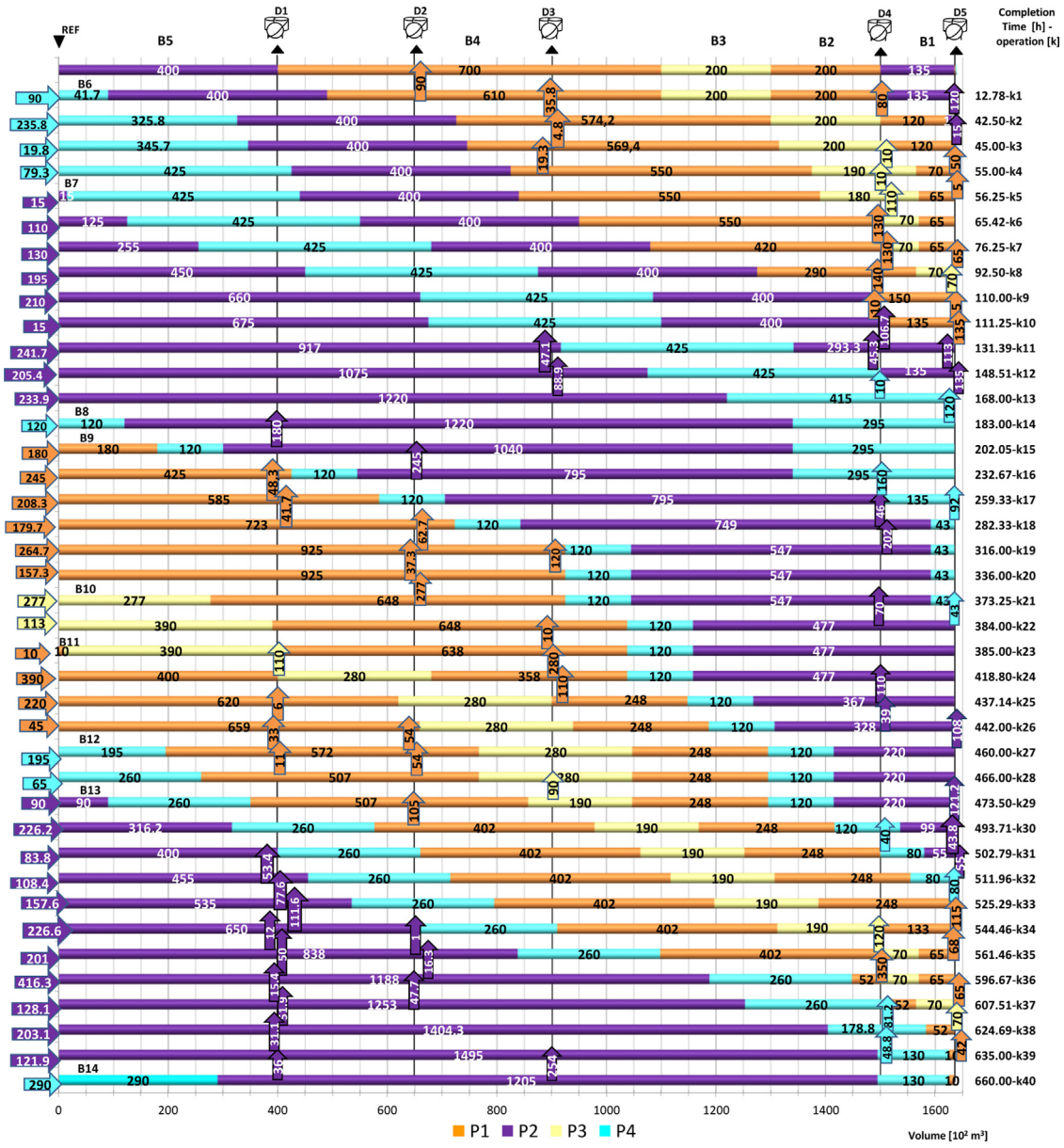

Fig. 7. Detailed delivery schedule obtained with the new MINLP formulation.

The variation of the flow rate in each pipeline segment is contrasted against the first MILP solution in the graphs of Fig. 8. As expected, the MINLP solution demonstrates a more stable behavior, which avoids keeping high flow rates during long periods of time. For instance, the last pipeline segment (D4–D5) works 15 h at its maximum flow rate (800 m^3/h), while the first MILP solution operates about 110 h at its maximum allowable value, as shown in the last graph of Fig. 8.

5.3. Example 3

Example 3 is introduced with the aim of reducing the computational effort required for solving the problem. In this example the planning horizon is divided into four weeks, so that an MINLP solution can be obtained for every week, individually. The monthly plan is then constructed by assembling the weekly detailed schedules, and can be compared with the one obtained in Example 2.

The first weekly problem includes the injection of batches B6 and B7, running from $t = 5.00$ h to $t = 168$ h. The second subproblem takes into account the injection of batches B8 and B9, operating from $t = 168$ h to $t = 336$ h. During the third weekly time interval, lots B10, B11 and B12 are injected, and finally the last subproblem involves the pumping of batches B13 and B14, from time $t = 466$ h to $t = 660$ h.

Although the initial MILP solutions for the weekly subproblems do not exactly match the first MILP solution of Example 2, the best detailed schedule obtained by applying the MINLP formulation separately is approximately the same as the one obtained when the monthly horizon is tackled all at once. The operation cost is merely increased by 0.02% due to slight changes in the flow rates of some operations, particularly in the segment D1–D2 during operations k_{19}, k_{20}, k_{38} and k_{39}. The other remarkable fact is the CPU time required. Adding the CPU times for every weekly schedule, a total of 99.2 s are required, about 186 times less than the CPU time needed for solving the MINLP formulation for the whole month.

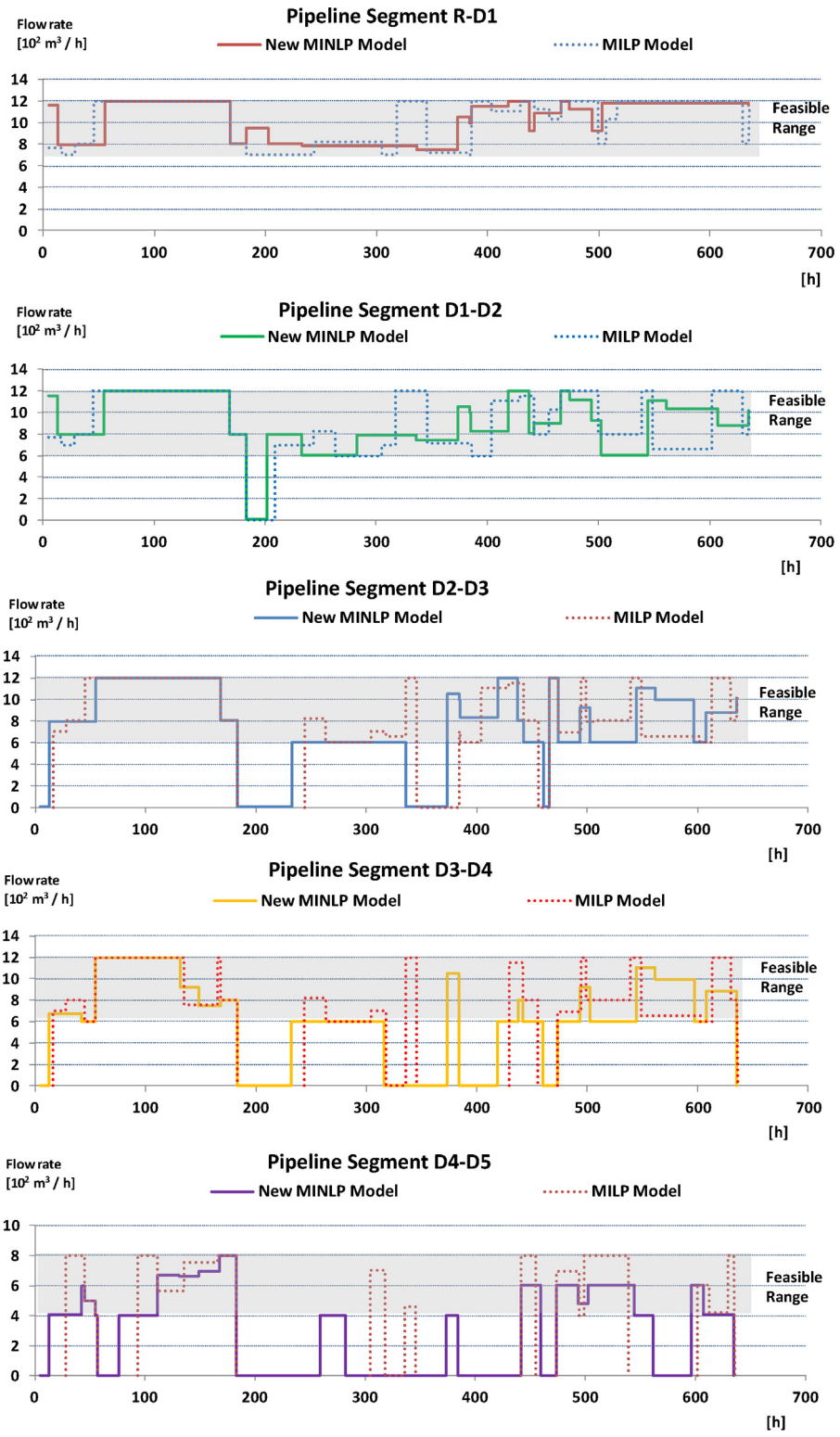

Fig. 8. Flow-rate variation in every pipeline segment, comparing the first MILP solution with the final MINLP result.

6. Conclusions

A new MINLP mathematical formulation for the detailed scheduling of single source pipelines with multiple depots has been developed. The problem constraints include an implicit nonlinear equation to estimate *the pump power required for transporting products into the pipeline*. The major difficulty of this kind of problems is the non-convexity, because it hinders the program convergence. We find out that DICOPT constitutes a useful tool for solving this large-scale scheduling problem. By defining an appropriate solution strategy to facilitate the problem convergence, the proposed model shows a good performance.

Since the CPU time required for solving the monthly plan is considerable, an alternative solution scheme sequentially solving four

weekly problems is proposed. The MINLP formulation is successfully applied to a real-world case study, reducing the total operation cost by 12.5% with regards to a previous approach only focused on restart/stoppage costs (Cafaro et al., 2012). Moreover, contrasting the detailed schedules, a more stable flow rate profile is achieved for every pipeline segment over the planning horizon.

Acknowledgments

Financial support received from FONCyT-ANPCyT under Grant PICT 1073, from CONICET under Grant PIP 2221, and from Universidad Nacional del Litoral under CAI+D is fully appreciated.

References

Bernoulli D. Hydrodynamica: sive de viribus et motibus fluidorum commentarii. Strasbourgh, France: Johann Reinhold Dulsseker; 1738.
Boschetto SN, Magatão L, Brondani WM, Neves-Jr F, Arruda LVR, Barbosa-Póvoa APFD, et al. An operational scheduling model to product distribution through a pipeline network. Ind Eng Chem Res 2010;49:5661–82.
Brooke A, Kendrick D, Meeraus A, Raman R. GAMS – A User's Guide. Washington, DC: GAMS Development Corporation; 2006.
Cafaro DC, Cerdá J. Optimal scheduling of multiproduct pipeline systems using a non-discrete MILP formulation. Comput Chem Eng 2004;28:2053–68.
Cafaro DC, Cerdá J. Dynamic scheduling of multiproduct pipelines with multiple delivery due dates. Comput Chem Eng 2008;32:728–53.
Cafaro DC, Cerdá J. A rigorous mathematical formulation for the scheduling of tree-structure pipeline networks. Ind Eng Chem Res 2011;50:5064–85.
Cafaro DC, Cerdá J. Rigorous scheduling of mesh-structure refined petroleum pipeline networks. Comput Chem Eng 2012;38:185–203.
Cafaro VG, Cafaro DC, Méndez CA, Cerdá J. Detailed scheduling of operations in single-source refined products pipelines. Ind Eng Chem Res 2011;50:6240–59.
Cafaro VG, Cafaro DC, Méndez CA, Cerdá J. Detailed scheduling of single-source pipelines with simultaneous deliveries to multiple offtake stations. Ind Eng Chem Res 2012;51:6145–65.
Cafaro VG, Cafaro DC, Cerdá J. Improving the mathematical formulation for the detailed scheduling of refined products pipelines by accounting for flow rate dependent pumping costs. Annals 42 JAIIO – SII 2013 2013: 24–35.
Castro PM. Optimal scheduling of pipeline systems with a resource-task network continuous-time formulation. Ind Eng Chem Res 2010;49:11491–505.
Colebrook CF, White CM. Experiments with fluid friction in roughened pipes. Proc R Soc Lond Ser A: Math Phys Sci 1937;161(906):367–81.
Darcy H. Recherches Experimentales Relatives au Mouvement de L'Eau dans les Tuyaux. Paris, France: Mallet-Bachelier; 1857.
Durán MA, Grossmann IE. An outer-approximation algorithm for a class of mixed-integer nonlinear programs. Math Program 1986;36:307–39.
García-Sánchez A, Arreche LM, Ortega-Mier M. Combining simulation and tabu search for oil-derivatives pipeline scheduling. Stud Comput Intell 2008;128:301–25.
Hane CA, Ratliff HD. Sequencing inputs to multi-commodity pipelines. Ann Oper Res 1995;57:73–101.
Herrán A, de la Cruz JM, de Andrés B. A mathematical model for planning transportation of multiple petroleum products in a multi-pipeline system. Comput Chem Eng 2010;34:401–13.
Lopes TMT, Ciré AA, de Souza CC, Moura AV. A hybrid model for a multiproduct pipeline planning and scheduling problem. Constraints 2010;15:151–89.
Miesner TO, Leffler WL. Oil & Gas Pipelines in Nontechnical Language. Tulsa, USA: Pennwell; 2006.
MirHassani SA, Jahromi HF. Scheduling multi-product tree-structure pipelines. Comput Chem Eng 2011;35:165–76.
Moody LF. Friction factors for pipe flow. Trans ASME 1944;66:671–84.
Neves-Jr F, Magatão L, Stebel SL, Boschetto SN, Felizari LC, Czaikowski DI, et al. An efficient approach to the operational scheduling of a real-world pipeline network. Comput Aided Chem Eng 2007;24:697–702.
Rejowski R, Pinto JM. Scheduling of a multiproduct pipeline system. Comput Chem Eng 2003;27:1229–46.
Rejowski R, Pinto JM. Efficient MILP formulations and valid cuts for multiproduct pipeline scheduling. Comput Chem Eng 2004;28:1511–28.
Rejowski R, Pinto JM. A rigorous MINLP for the simultaneous scheduling and operation of multiproduct pipeline systems. Comput Aided Chem Eng 2005;20(C):1063–8.
Rejowski R, Pinto JM. A novel continuous time representation for the scheduling of pipeline systems with pumping yield rate constraints. Comput Chem Eng 2008;32:1042–66.
Relvas S, Matos HA, Barbosa-Póvoa APFD, Fialho J, Pinheiro AS. Pipeline scheduling and inventory management of a multiproduct distribution oil system. Ind Eng Chem Res 2006;45:7841–55.